

## Nanodisc Films for Membrane Protein Studies by Neutron Reflection: Effect of the Protein Scaffold Choice

Nicolas Bertram,<sup>†</sup> Tomas Laursen,<sup>‡,#</sup> Robert Barker,<sup>§</sup> Krutika Bavishi,<sup>‡,#</sup> Birger Lindberg Møller,<sup>‡,||,⊥,#</sup> and Marité Cárdenas<sup>\*,†,||,#</sup>

<sup>†</sup>Nano-Science Center and Department of Chemistry, Faculty of Science, University of Copenhagen, DK-2200, Copenhagen, Denmark

<sup>‡</sup>Plant Biochemistry Laboratory and <sup>||</sup>VILLUM research center of excellence “Plant Plasticity”, Department of Plant and Environmental Science, Faculty of Science, University of Copenhagen, DK-1871 Frederiksberg C, Denmark

<sup>§</sup>Institut Laue Langevin, 71 Avenue des Martyrs – CS 20156, 38042 Grenoble Cedex 9, France

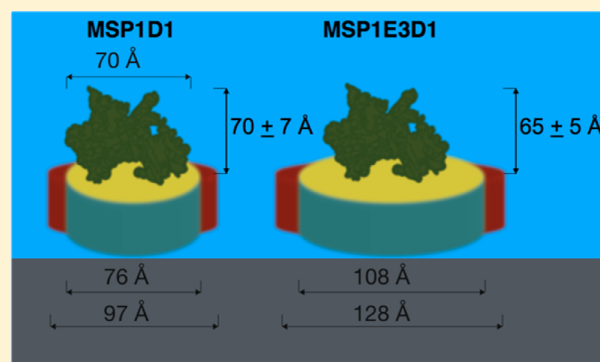
<sup>⊥</sup>Carlsberg Laboratory, 10 Gamle Carlsberg Vej, DK-1799 Copenhagen V, Denmark

<sup>||</sup>Malmö University, Department of Biomedical Sciences and Biofilm—Research Centre for Biointerfaces, Health & Society, 20506 Malmö, Sweden

<sup>#</sup>Center of Synthetic Biology “bioSYNergy”, University of Copenhagen, 40 Thorvaldsensvej, DK-1871 Frederiksberg C, Denmark

### Supporting Information

**ABSTRACT:** Nanodisc films are a promising approach to study the equilibrium conformation of membrane bound proteins in native-like environment. Here we compare nanodisc formation for NADPH-dependent cytochrome P450 oxidoreductase (POR) using two different scaffold proteins, MSP1D1 and MSP1E3D1. Despite the increased stability of POR loaded MSP1E3D1 based nanodiscs in comparison to MSP1D1 based nanodiscs, neutron reflection at the silicon–solution interface showed that POR loaded MSP1E3D1 based nanodisc films had poor surface coverage. This was the case, even when incubation was carried out under conditions that typically gave high coverage for empty nanodiscs. The low surface coverage affects the embedded POR coverage in the nanodisc film and limits the structural information that can be extracted from membrane bound proteins within them. Thus, nanodisc reconstitution on the smaller scaffold proteins is necessary for structural studies of membrane bound proteins in nanodisc films.



## INTRODUCTION

The function and structure of membrane proteins remain one of the most challenging and exciting areas of molecular biology. The eukaryotic cytochrome P450 (CYP) enzyme superfamily is an interesting class of membrane proteins. In addition to their key functions in primary metabolism, they are catalyzing the synthesis of numerous classes of bioactive compounds in plants and in the metabolism of xenobiotics including drugs in humans. Microsomal CYPs require electron donation from an NADPH-dependent cytochrome P450 oxidoreductase (POR) to complete their catalytic cycle.<sup>1</sup> Detergent solubilization and isolation of POR has been shown to alter its functional properties including a decrease in flavin stability.<sup>2</sup> In vitro built lipid membranes can be used to mimic the cellular membrane and several lipid membrane based approaches exist including the apolipoprotein based nanodisc<sup>3,4</sup> and the polymer based nanodisc,<sup>5,6</sup> among others.<sup>7</sup> In situ studies of membrane proteins incorporated into nanodiscs have previously been performed by small angle scattering<sup>8</sup> and neutron reflection.<sup>9</sup> Still, challenges remain in terms of the loaded protein nanodisc

yield, number of membrane proteins loaded per nanodisc, and functionality of the reconstituted membrane protein.<sup>2</sup> Some factors to consider are the lipid properties in terms of fluidity, bilayer thickness, and charge, as well as the choice of nanodisc diameter.<sup>10</sup> The use of small MSP1D1 nanodiscs resulted in a low yield of POR loading<sup>9</sup> which motivated the reconstitution into larger scaffold proteins. In the current study, we have investigated the importance of a number of different parameters to better understand the behavior of the nanodisc system. POR was reconstituted in nanodiscs using the scaffold protein MSP1E3D1, which forms nanodiscs of 13 nm in diameter compared to 10 nm from MSP1D1 derived nanodiscs.<sup>11</sup> Empty MSP1E3D1 based nanodisc films were produced and characterized using either pure 1,2-dimyristoyl-*sn*-glycero-3-phosphocholine (DMPC) or 3:1 molar ratio mixtures of DMPC and 1,2-dimyristoyl-*sn*-glycero-3-phosphoglycerol

Received: March 19, 2015

Revised: July 5, 2015

Published: July 14, 2015

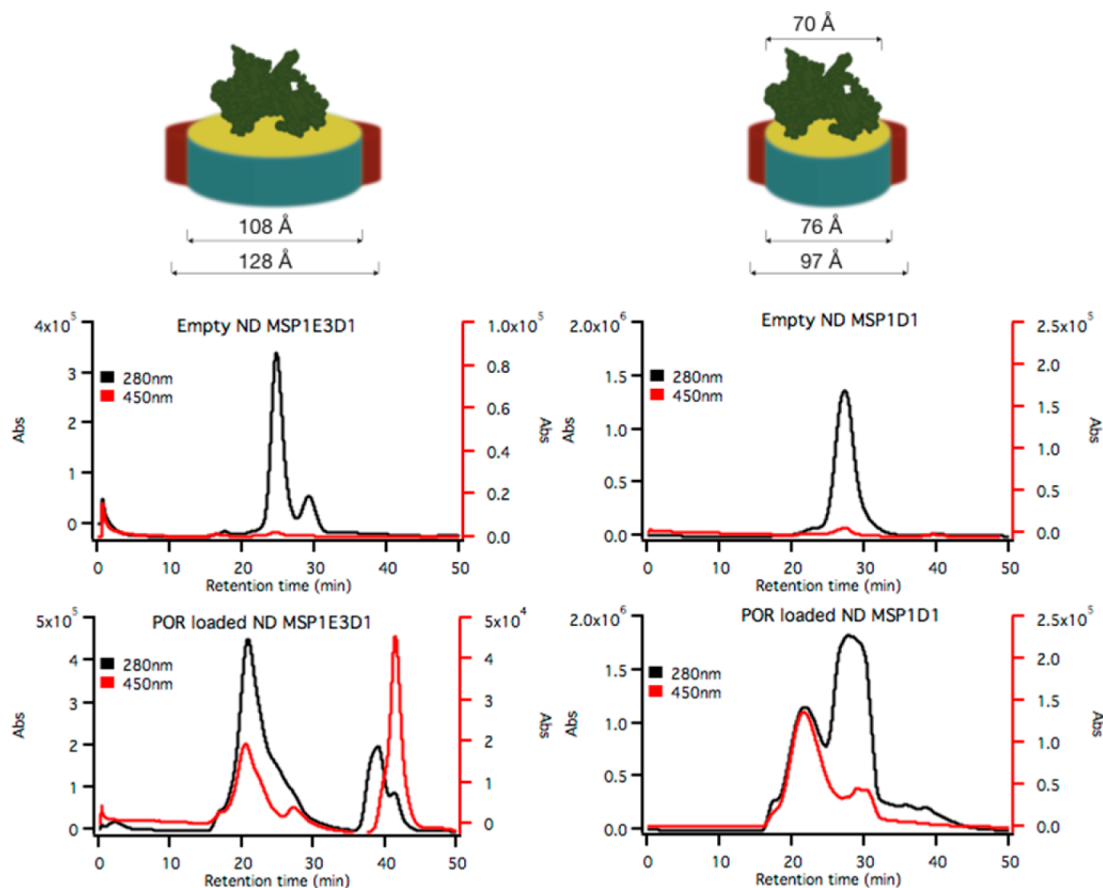


**Figure 1.** HPLC chromatograms for POR loaded and empty DMPC-MSP1D1, DMPC-MSP1E3D1 nanodisc. Schematics of nanodisc with and without the POR protein are shown to scale, using the dimensions reported in refs 1,4. The nanodiscs are drawn using red color to represent the protein belt, while yellow and blue colors represent the hydrophilic and hydrophobic regions of the lipid bilayer, respectively.

(DMPG) at 14 °C. The reversibility of melting the lipid bilayer was investigated because the lipid state might be important for POR function. Finally, we produced and characterized the POR loaded nanodiscs. The challenges involved in studying conformational changes in these films are discussed.

## EXPERIMENTAL SECTION

**Materials and Methods.** The scaffold proteins used were MSP1D1 and MSP1E3D1, expressed and purified according to Bayburt et al.<sup>12</sup> DMPC and DMPG were purchased from Avanti Polar Lipids Inc. and used as received. Tris and NaCl (Sigma-Aldrich) were dissolved in Milli-Q water or D<sub>2</sub>O provided by the Institute Laue Langevin (ILL, France) or Rutherford Appleton Laboratory (ISIS, U.K.) and adjusted to pH 7.4 using HCl. POR was expressed and purified following previously published protocols.<sup>9</sup> Nanodiscs were prepared as described elsewhere,<sup>9</sup> using lipid to MSP ratios depending on the scaffold protein: 80:1 and 120:1 for MSP1D1 and MSP1E3D1, respectively. We used DMPC as well as DMPC:DMPG at a molar ratio of 3:1 in the preparation of both empty and POR loaded nanodiscs. To optimize the reconstitution efficiency, POR loaded MSP1D1 nanodiscs were assembled with a 10-fold molar excess of nanodiscs to POR compared to a 3-fold molar excess of MSP1E3D1 nanodiscs. Detergent was removed by overnight adsorption to Biobeads SM-2 (Biorad) followed by fractionation by gel filtration (flow rate: 0.5 mL/min) on a preparative HPLC (Shimadzu) equipped with a Superdex 200 HR 10/30 column (Amersham Pharmacia Biotech, diameter: 10 mm, height: 300 mm). The elution of total protein and POR was monitored by absorbance recordings at 280 and 450 nm, respectively. Two or three 0.5 mL fractions were collected at the beginning of the elution of the relevant nanodisc peak (retention

times 20–22 min), and combined to use for further studies. The fractions were chosen to avoid contamination of the POR loaded nanodiscs with empty nanodiscs. Nanodisc samples were kept at –80 °C until used. This is a routine procedure in our laboratory that preserves the functional and structural integrity of the nanodiscs as demonstrated in the [Supporting Information](#). The Si/SiO<sub>2</sub> substrates were pretreated by soaking in Piranha solution (50% H<sub>2</sub>O:40% H<sub>2</sub>SO<sub>4</sub>:10% H<sub>2</sub>O<sub>2</sub> at 80 °C for 10 min) to obtain hydrophilic properties. Nanodisc solutions in H<sub>2</sub>O based buffer (20 mM Tris, 100 mM NaCl, pH 7.4) were injected in to the liquid flow cell at a concentration of 45 or 200 nM (as calculated from the total protein content) at 14 °C. The solution was left in the cell to equilibrate for either 3–4 h or 6–7 h, prior to extensive rinsing with buffer at 0.5 mL/min.

**Neutron Reflectivity (NR).** Neutrons are scattered by the nucleus of an atom. The ability to scatter neutrons depends on both the isotope and atomic number of an element, and is quantified by the scattering length density (SLD) calculated by the sum of  $b_i$ , the coherent scattering length of each nuclei  $i$  divided by a given volume. In NR, the intensity of specular (mirror-like) reflected neutrons ( $R$ ) is measured as a function of the scattering vector perpendicular to the interface ( $Q = 4\pi\sin(\theta)/\lambda$ , where  $\theta$  is the angle of reflection and  $\lambda$  is the neutron wavelength).  $R$  relates to the SLD of a material via an inverse Fourier transformation.<sup>13</sup> Specular NR provides the averaged composition and structure of the interfacial material along an axis perpendicular to the surface. The advantage of using neutrons in biological systems comes from the different scattering lengths of the isotopes hydrogen and deuterium,<sup>14</sup> which allows for contrast variation by deuterium substitution for hydrogen. NR profiles were analyzed by fitting a simulated reflectivity curve of a model structure to the experimental data using the software RasCAL.<sup>15</sup> This software uses the

Abeles optical matrix method<sup>16</sup> to calculate the reflectivity of thin layers and enables simultaneous fitting of data sets with different isotopic compositions. Fit parameters are adjusted via a least-squares minimization that reduces the differences between the model reflectivity and the data. Model to experimental data fitting errors were obtained using RasCAL's "bootstrap" error analysis function,<sup>17</sup> in which the original data set is resampled and these new data sets fitted via the same methods described earlier. The parameter value distributions obtained across these fits were used to estimate errors that were propagated through the calculations of the derived parameters according to standard error treatment methods. The NR was performed at three beamlines: D17<sup>18</sup> (ILL), SURF (ISIS),<sup>19</sup> and INTER (ISIS).

The clean Si/SiO<sub>2</sub> substrate was precharacterized in order to fit the thickness, roughness, and solvent content of the SiO<sub>2</sub> layer. The DMPC or DMPC/DMPG nanodiscs were modeled assuming that each nanodisc contained 320 phospholipids (the reported value of 160 lipids/scaffold protein<sup>11</sup> was used in this calculation) and using constant volumes of the lipids<sup>20</sup> and MSP.<sup>11</sup> The lipids and the two MSP proteins were modeled as cylinders and as a uniform belt with equal thickness to that of the lipid bilayer tails. The nanodisc model includes the solvent filling the space above the protein scaffold that is not occupied by lipids, respectively. This analysis gave a SLD of  $5.41 \times 10^{-7} \text{ \AA}^{-2}$  and  $1.04 \times 10^{-6} \text{ \AA}^{-2}$  for nanodiscs in H<sub>2</sub>O and D<sub>2</sub>O, respectively. The empty nanodisc film was modeled as a single layer where the thickness, coverage, and roughness were fitted separately. The POR loaded nanodisc film was modeled as two independent layers where the thickness, coverage, and roughness of each layer were fitted separately: one of the layers corresponds to the nanodiscs (scaffold protein and lipids) and the other layer corresponds to the membrane associated protein (POR). As is common for supported lipid bilayers,<sup>21,22</sup> a thin solvent layer between the nanodisc and the solid substrate was required to properly fit the data.<sup>20</sup> The thickness of the solvent layer is of the same order of magnitude as the substrate roughness and represents the water trapped within the roughness of the surface, too small to incorporate lipid head groups. All data sets were fitted simultaneously with an independent set of layers attributed to each sample.

## RESULTS AND DISCUSSION

The self-assembly of POR loaded nanodiscs using DMPC and either of the membrane scaffold proteins MSP1D1 or MSP1E3D1 was monitored by HPLC analysis (Figure 1). At 280 nm, both the presence of the scaffold protein as well as the POR is detected, while the absorption of the POR associated flavin coenzymes at 450 nm allows for specific monitoring of the presence of POR in the nanodisc containing sample preparation. The preparation of empty nanodiscs is well-defined as monitored by minimal smearing and high monodispersity. The POR loaded nanodiscs are more challenging to prepare and typically show a widened elution peak. Constructs eluting earlier than 30 min were attributed to a mixture of empty and POR loaded nanodiscs. For the MSP1E3D1 and MSP1D1 based nanodiscs, the POR loaded discs eluted at 20.5 and 21.5 min, while empty nanodiscs eluted at 25 and 27 min, respectively. Peaks appearing after 35 min were considered unbound material, representing single copies or fractions of MPs, MSPs in combination with unknown numbers of lipids and free flavins. The elution profiles obtained for the empty nanodiscs were in agreement with previously reported data.<sup>23</sup> Reconstitution of POR in MSP1E3D1 nanodiscs resulted in a mixture of loaded and empty discs and the elution profile of these two species partly overlapped. Deconvolution of the absorption profile of these peaks showed that there was no significant contribution from empty nanodisc peak in the collected fractions for POR loaded nanodiscs (data

not shown), although it is not possible to completely disregard the presence of empty nanodiscs in the preparation used for NR experiments. Finally, previous work by our group showed that POR oligomers coelute with POR loaded nanodiscs when reconstituted using MSP1D1 while this does not occur for MSP1E3D1.<sup>2</sup> Thus, POR reconstitution into nanodiscs was facilitated by use of the MSP1E3D1 scaffold protein, which might be due to the greater lipid bilayer area ( $8900 \text{ \AA}^2$  compared to  $4400 \text{ \AA}^2$  for MSP1E3D1 and MSP1D1, respectively<sup>11</sup>) that minimizes POR–MSP interactions and possibly stabilizes the POR loaded nanodiscs, and minimizes the formation of oligomers in the detergent free matrix.<sup>2</sup>

Experiments were carried out to study the formation of MSP1E3D1 based nanodiscs with the aim of optimizing the surface coverage and structurally characterize these discs. Different batch preparations of nanodiscs were used to characterize films of empty DMPC nanodiscs formed at a concentration of either 45 or 200 nM at 14 °C (Figure 2). Due to uncertainties with respect to the exact dimensions of the discs,<sup>11</sup> SLD values of each sample were fitted for the nanodisc layers in each contrast as common parameters among the different samples and gave  $(5.6 \pm 0.6) \times 10^{-7} \text{ \AA}^{-2}$  and  $(1.00 \pm 0.07) \times 10^{-6} \text{ \AA}^{-2}$  for nanodiscs in H<sub>2</sub>O and D<sub>2</sub>O, respectively.

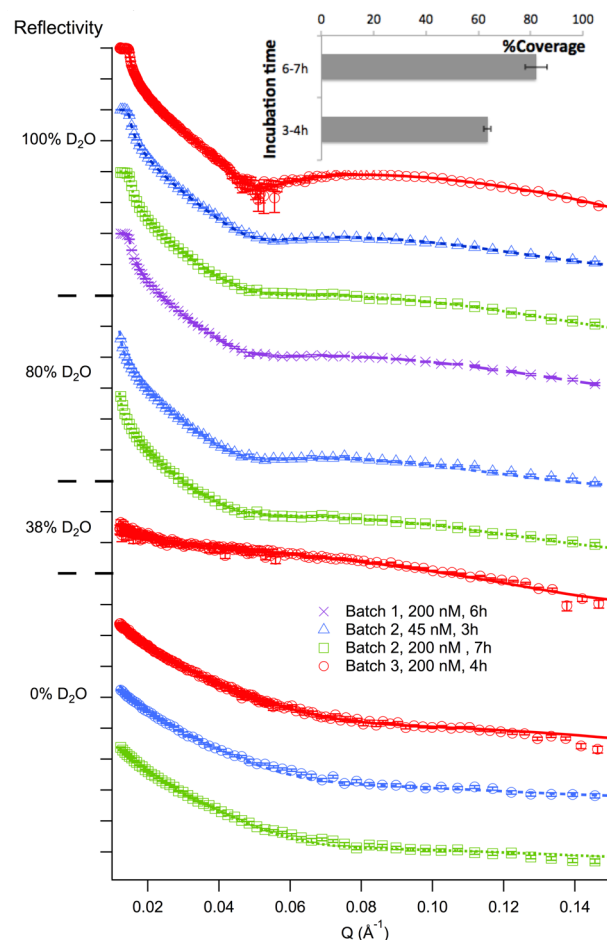


**Figure 2.** Neutron reflectivity profiles for DMPC-MSP1E3D1 based nanodisc films formed after different incubation times and nanodisc concentrations. Nanodiscs were modeled as a single layer that is  $38 \pm 3 \text{ \AA}$  thick with  $8 \pm 2 \text{ \AA}$  roughness. A clear dependency of the surface coverage with incubation time is observed (inset). Typical SiO<sub>2</sub> layers were  $9 \pm 3 \text{ \AA}$  thick with a  $4 \pm 2 \text{ \AA}$  roughness.

This is in excellent agreement with the calculated values based on our model (see [Experimental Section](#)).

MSP1E3D1 based nanodiscs prepared using a mixture of DMPC/DMPG (1:3 molar ratio) were used to form films at 200 nM after a 6 h incubation at 14 °C ([Figure 3](#)). The data

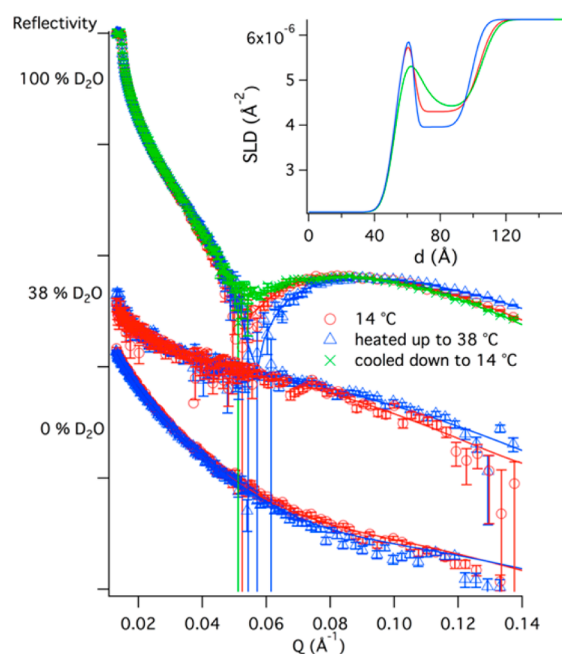


**Figure 3.** Neutron reflectivity profiles for DMPC/DMPG-MSP1E3D1 after 6 h incubation time at 14 °C, and upon heating the film to 38 °C and recooling to 14 °C. The SLD for the best fits (inset) show that the nanodisc film becomes thinner and increases in coverage upon heating, and this effect is semireversible. For clarity, in the latter case only the D<sub>2</sub>O contrast is shown. Typical SiO<sub>2</sub> layers were 5 ± 1 Å thick with 3 ± 1 Å roughness.

obtained were fitted using the SLD values calculated for DMPC nanodiscs, because the SLD of PC and PG head groups does not differ significantly.<sup>20</sup> The nanodisc layer thickness was 40 ± 1 Å and presented a relatively high interfacial roughness of 7 ± 1 Å. Thus, the overall nanodisc film structure does not seem to be affected by the presence of DMPG lipids, although the surface coverage was significantly lower in this case (38 ± 1%). This is probably due to electrostatic repulsions between the negatively charged SiO<sub>2</sub> surface and the nanodiscs.

The NR data analysis suggests that the gel-phase nanodisc layer was 38 ± 3 Å thick, in agreement with the thickness found for MSP1D1 based nanodiscs under similar conditions,<sup>9</sup> and the gel-phase DMPC bilayer thickness.<sup>24</sup> Thus, the scaffold protein does not affect the conformation and packing of DMPC molecules in the bilayer patch. However, the interfacial roughness was significantly higher for the MSP1E3D1 compared to the MSP1D1 based nanodisc films prepared using similar substrates and experimental conditions. This suggests that the larger MSP1E3D1 nanodiscs are either more flexible or less organized at the interface, or they present a less well-defined bilayer patch in the nanodisc. With respect to nanodisc surface coverage, similar results were found for adsorption at 45 and 200 nM. A clear correlation between coverage and incubation time was observed giving the high ~80% coverage only following the extended 6–7 h incubation period. Thus, the nanodisc layer either slowly rearranges over time so that more nanodiscs can diffuse and adsorb to the

surface, or with time the nanodisc layer becomes more stable against rinsing with buffer.

Upon heating the nanodisc film to 38 °C, well above the melting temperature of DMPC, the nanodisc layer thinned to 35 ± 1 Å and expanded by 7 ± 1 v/v% with no change in the film roughness (6 ± 1 Å). This is as expected following the melting of the lipid bilayer in the nanodisc.<sup>20</sup> No significant changes in the roughness of the nanodisc layer were observed which is in contrast to the results obtained with MSP1D1 based nanodiscs.<sup>20</sup> This suggests that the organization of the MSP1E3D1 based nanodisc films is independent of the lipid phase. We expected higher roughness given the requirement for hydrophobic matching between the scaffold protein and the lipid patch and the varied thickness of free supported DMPC bilayers in the gel (42–43 Å)<sup>25</sup> and liquid crystalline (34–36 Å)<sup>25,26</sup> phases. Most likely, the larger flexibility of the MSP1E3D1 based nanodiscs masks subtle changes in the bilayer patch organization within these films. Finally, the overall thickness (41 ± 2 Å), roughness (7 ± 2 Å), and surface coverage (36 ± 2%) seemed reversible upon recooling to 14 °C. The reflectivity profile, though, did not fully reproduce the NR profile prior to heating, thus indicating that nanodiscs partly disassemble into their components within the film upon heating.

Our data suggests that high nanodisc surface coverage can be obtained for MSP1E3D1 based nanodiscs upon adsorption above 45 nM and 6–7 h incubation time at 14 °C. We produced three POR loaded MSP1E3D1 DMPC nanodisc films under these conditions and characterized them by NR ([Figure 4](#)). The overall structure of the POR nanodisc film is similar to that obtained for MSP1D1-based nanodiscs, for which the lipid bilayer patch is situated flat on the silicon surface with the disc inserted POR specifically protruding into the solution.<sup>9</sup> The structure of the nanodisc layer was not significantly affected by the presence of POR. This is not surprising given that the transmembrane helix of the POR is predicted to replace only 5 lipid molecules with minimal effects on the SLD of the nanodisc.<sup>9</sup> On the other hand, the coverage of the POR loaded nanodisc layer was harder to reproduce than for empty nanodiscs, and typical surface coverage ranged between 40 and 60 v/v% corresponding to a protein coverage ranging from 3% to 10%. From this, we estimate that 80 ± 20% of the nanodiscs contained one POR/nanodisc except for the preparation that gave high surface coverage (batch 1). In this case, at least 50% of the nanodiscs contained 2 POR/nanodisc (150 ± 30%). The presence of nonreconstituted dimers and oligomers in solution have been identified previously by native PAGE,<sup>2</sup> and might occur in some of our samples (there are slight absorption shoulders in the shape of the HPLC elution profile during sample fractionation, [Figure 1](#)). For MSP1D1 based nanodiscs, the POR/nanodisc ratio was 90 ± 20% and this was confirmed by single molecule confocal fluorescence microscopy.<sup>9</sup> Thus, POR loaded nanodiscs show strong preferential adsorption to adsorb on silicon surfaces over non reconstituted POR oligomers which could potentially be present in the sample. The high affinity of lipids to adsorb on hydrophilic surfaces and the fact that POR enzyme protrudes on a single side of each nanodisc may guide the specific adsorption pattern. This is the great advantage of nanodisc film and NR over bulk scattering techniques, for which the purity of the sample is a major limitation in the data analysis.

The low POR surface coverage arises from the larger area that each nanodisc occupies with respect to the POR protein.

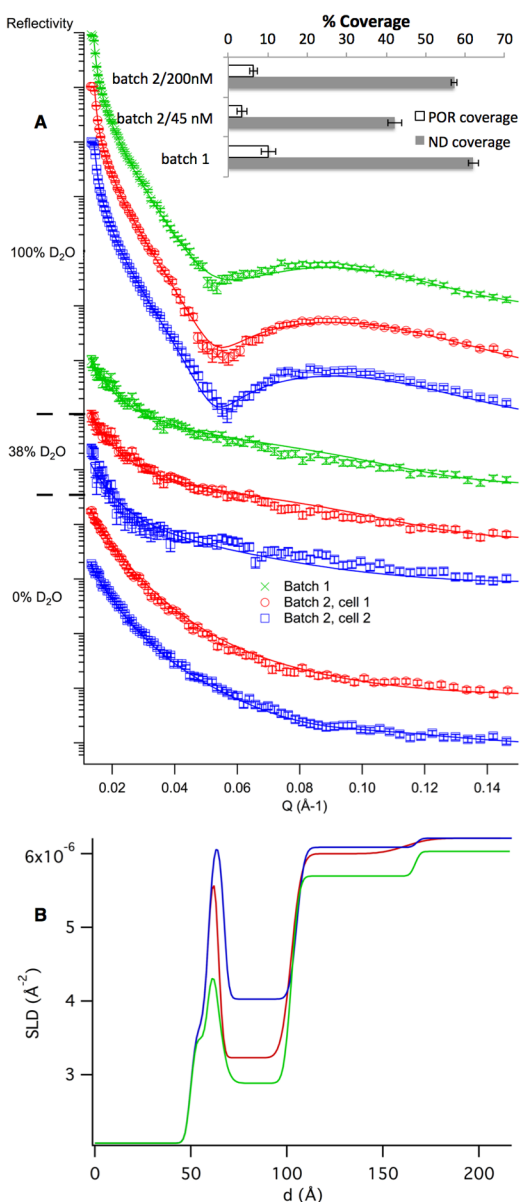


**Figure 4.** Neutron reflectivity profiles for POR loaded DMPC-MSP1E3D1 (200 nM) after 6–7 h incubation time at 14 °C (A) and SLD profiles for the best fits (for clarity, only shown for the D<sub>2</sub>O contrast) (B). Nanodiscs were modeled as a single layer with a thickness of  $39 \pm 1$  Å and with a roughness of  $4 \pm 1$  Å. POR was modeled as a single layer of  $65 \pm 5$  Å thickness and a roughness of  $6 \pm 4$  Å. Despite the extended incubation period, the nanodisc and POR surface coverage remained low, ranging between 50% and 60% and 3%, respectively, therefore limiting any conformational studies of the membrane protein in the discs. Only in one case (batch 1) was the POR coverage comparable to that obtained for the MSP1D1 nanodiscs.<sup>9</sup> However, this particular sample seemed to contain more than one POR per nanodisc (Inset in A). Typical SiO<sub>2</sub> layers were  $9 \pm 1$  Å thick with  $3 \pm 1$  Å roughness. The various batches represent different preparations.

In MSP1E3D1 based nanodiscs, POR accounts for  $\sim 13\%$  of the disc surface area, whereas the corresponding value for nanodiscs prepared from MSP1D1 is  $\sim 35\%$ . This difference in relative area occupied by POR per nanodisc in combination with the low surface coverage is enough to reach the limit of useful detection using NR. This limits the extent of structural

information that can be obtained from the POR loaded nanodisc films in the larger MSP1E3D1. Indeed, the overall protein thickness cannot be obtained with any certainty for POR coverage below 4 v/v%. The use of smaller MSP1D1 is necessary to obtain structural information on membrane proteins embedded in nanodisc films despite the lower yield of POR loaded nanodiscs. A possible explanation for the lower coverage in POR loaded MSP1E3D1 based nanodisc films is the greater conformational flexibility of the nanodisc as a whole, manifested by formation of rougher nanodisc films as compared to those formed from MSP1D1 based nanodiscs (evident for empty nanodisc).<sup>9</sup> Greater flexibility of the conformation of the nanodisc raises the energy barrier for dense film formation due to difficulties to create sufficient contact points with the surface. This increased roughness also reduces the resolution of the information that can be obtained about the POR due to propagation of this roughness in to the protein layer. Finally, similar results were obtained for POR loaded MSP1E3D1 based nanodiscs for which DMPC-DMPG mixtures were used (data not shown).

## CONCLUSIONS

DMPC or DMPC/DMPG MSP1E3D1 based nanodisc films show comparable structural characteristics to those made from the smaller MSP1D1 (Figures 2, 3, and ref 20). Despite the higher yield of POR loaded nanodisc in MSP1E3D1 (Figure 1), the lower ratio of area occupied by POR in the nanodisc combined with the lower surface coverage (Figure 4) limits the extent of structural information that can be obtained using NR. Thus, it is of extreme importance to choose a small scaffold protein such as MSP1D1 for obtaining structurally relevant information from NR experiments. However, reconstitution of POR in MSP1D1 nanodiscs does not properly support membrane association<sup>9</sup> compared to MSP1E3D1.<sup>2</sup> Optimization of the POR reconstitution procedure in other intermediate scaffold proteins such as MSP1E1 and MSPE2<sup>23</sup> offers the opportunity to obtain proper structural data by NR.

## ASSOCIATED CONTENT

### Supporting Information

Functional and structural assays after freezing to  $-80$  °C are proof of nanodisc integrity. The Supporting Information is available free of charge on the ACS Publications website at DOI: 10.1021/acs.langmuir.5b00936.

## AUTHOR INFORMATION

### Corresponding Author

\*E-mail: marite.cardenas@mah.se, cardenas@nano.ku.dk.

### Author Contributions

Nicolas Bertram and Tomas Laursen have contributed equally to this work. TL, NB, and KB performed reconstitution of the nanodiscs. NB, TL, RB, BLM, and MC planned all experiments. NB, RB, and MC performed NR experiments. NB and MC analyzed the data. All authors contributed to the discussion and writing of this work.

### Notes

The authors declare no competing financial interest.

## ACKNOWLEDGMENTS

We acknowledge financial support from DANSCATT Centre (Danish government), the ILL stagiare program, the Swedish Research Council (MC), a grant from the VILLUM research

center of excellence “Plant Plasticity”, by the Center for Synthetic Biology “bioSYnergy” supported by the UCPH Excellence Program for Interdisciplinary Research, the ‘P4FIFTY’ People Programme (Marie Curie Actions) of the European Union’s Seventh Framework Programme FP7/2007–2013/ under REA Grant agreement no. 289217 (K.B and B.L.M.), and by an ERC Advanced Grant to BLM (ERC-2012-ADG\_20120314, Project No: 323034). Thanks to ILL and ISIS for allocated beamtime and to Maximilian Skoda and Arwel Hughes (ISIS) for local support.

## REFERENCES

- (1) Laursen, T.; Jensen, K.; Moller, B. L. Conformational changes of the NADPH-dependent cytochrome P450 reductase in the course of electron transfer to cytochromes P450. *Biochim. Biophys. Acta, Proteins Proteomics* **2011**, *1814* (1), 132–8.
- (2) Laursen, T.; Singha, A.; Rantzau, N.; Tutkus, M.; Borch, J.; Hedegard, P.; Stamou, D.; Moller, B. L.; Hatzakis, N. S. Single Molecule Activity Measurements of Cytochrome P450 Oxidoreductase Reveal the Existence of Two Discrete Functional States. *ACS Chem. Biol.* **2014**, *9*, 630–634.
- (3) Borch, J.; Hamann, T. The nanodisc: a novel tool for membrane protein studies. *Biol. Chem.* **2009**, *390* (8), 805–14.
- (4) Bayburt, T. H.; Sligar, S. G. Membrane protein assembly into Nanodiscs. *FEBS Lett.* **2010**, *584* (9), 1721–7.
- (5) Gorbenko, G. P.; Molotkovsky, J. G.; Kinnunen, P. K. J. Cytochrome c Interaction with Cardiolipin/Phosphatidylcholine Model Membranes: Effect of Cardiolipin Protonation. *Biophys. J.* **2006**, *90* (11), 4093–4103.
- (6) Trusova, V. M.; Gorbenko, G. P.; Molotkovsky, J. G.; Kinnunen, P. K. J. Cytochrome c-Lipid Interactions: New Insights from Resonance Energy Transfer. *Biophys. J.* **2010**, *99* (6), 1754–1763.
- (7) Warschawski, D. E.; Arnold, A. A.; Beaugrand, M.; Gravel, A.; Chartrand, E.; Marcotte, I. Choosing membrane mimetics for NMR structural studies of transmembrane proteins. *Biochim. Biophys. Acta, Biomembr.* **2011**, *1808* (8), 1957–74.
- (8) Kynde, S. A. R.; Skar-Gislinge, N.; Pedersen, M. C.; Midtgaard, S. R.; Simonsen, J. B.; Schweins, R.; Mortensen, K.; Arleth, L. Small-angle scattering gives direct structural information about a membrane protein inside a lipid environment. *Acta Crystallogr., Sect. D: Biol. Crystallogr.* **2014**, *70*, 371–383.
- (9) Wadsäter, M.; Laursen, T.; Singha, A.; Hatzakis, N. S.; Stamou, D.; Barker, R.; Mortensen, K.; Feidenhans'l, R.; Møller, B. L.; Cárdenas, M. Monitoring Shifts in the Conformation Equilibrium of the Membrane Protein Cytochrome P450 Reductase (POR) in Nanodiscs. *J. Biol. Chem.* **2012**, *287*, 34596–34603.
- (10) Lee, A. G. How lipids affect the activities of integral membrane proteins. *Biochim. Biophys. Acta, Biomembr.* **2004**, *1666* (1–2), 62–87.
- (11) Ritchie, T. K.; Grinkova, Y. V.; Bayburt, T. H.; Denisov, I. G.; Zolnerciks, J. K.; Atkins, W. M.; Sligar, S. G. Chapter 11 Reconstitution of Membrane Proteins in Phospholipid Bilayer Nanodiscs. *Methods Enzymol.* **2009**, *464*, 211–231.
- (12) Bayburt, T. H.; Grinkova, Y. V.; Sligar, S. G. Self-Assembly of Discoidal Phospholipid Bilayer Nanoparticles with Membrane Scaffold Proteins. *Nano Lett.* **2002**, *2*, 853–856.
- (13) Majkrzak, C. F.; Satija, S. K.; Berk, N. F.; Borchers, J. A.; Dura, J. A.; Ivkov, R.; O'Donovan, K. Neutron reflectometry at the NCNR. *Neutron News* **2001**, *12*, 25–29.
- (14) Jacrot, B. The study of biological structures by neutron scattering from solution. *Rep. Prog. Phys.* **1976**, *39*, 911–953.
- (15) Hughes, A. V. RasCAL. Sourceforge; <http://sourceforge.net/projects/rscl/>; accessed 2013.
- (16) Abeles, F. Sur la propagation des ondes electromagnetiques dans les milieux stratifiés. *Ann. Phys.* **1948**, *3*, 504–520.
- (17) Efron, B. Bootstrap methods: Another look at the jackknife. *Annals of Statistics* **1979**, *7*, 1–26.
- (18) Cubitt, R.; Fragneto, G. D17: the new reflectometer at the ILL. *Appl. Phys. A: Mater. Sci. Process.* **2002**, *74*, S329–S331.
- (19) Penfold, J.; Richardson, R. M.; Zorbakhsh, A.; Webster, J. R. P.; Bucknall, D. G.; Rennie, A. R.; Jones, R. A. L.; Cosgrove, T.; Thomas, R. K.; Higgins, J. S.; Fletcher, P. D. I.; Dickinson, E.; Roser, S. J.; McLure, I. A.; Hillman, A. R.; Richards, R. W.; Staples, E. J.; Burgess, A. N.; Simister, E. A.; White, J. W. Recent advances in the study of chemical surfaces and interfaces by specular neutron reflection. *J. Chem. Soc., Faraday Trans.* **1997**, *93* (22), 3899–3917.
- (20) Wadsäter, M.; Barker, R.; Mortensen, K.; Feidenhans'l, R.; Cárdenas, M. Effect of Phospholipid Composition and Phase on Nanodisc Films at the Solid–Liquid Interface as Studied by Neutron Reflectivity. *Langmuir* **2013**, *29* (9), 2871–2880.
- (21) Åkesson, A.; Lind, T.; Ehrlich, N.; Stamou, D.; Wacklin, H. P.; Cardenas, M. Composition and structure of mixed phospholipid supported bilayers formed by POPC and DPPC. *Soft Matter* **2012**, *8* (20), 5658–5665.
- (22) Koenig, B. W.; Krueger, S.; Orts, W. J.; Majkrzak, C. F.; Berk, N. F.; Silverton, J. V.; Gawrisch, K. Neutron Reflectivity and Atomic Force Microscopy Studies of a Lipid Bilayer in Water Adsorbed to the Surface of a Silicon Single Crystal. *Langmuir* **1996**, *12*, 1343–1350.
- (23) Denisov, I. G.; Grinkova, Y. V.; Lazarides, A. A.; Sligar, S. G. Directed self-assembly of monodisperse phospholipid bilayer nanodiscs with controlled size. *J. Am. Chem. Soc.* **2004**, *126* (11), 3477–3487.
- (24) Tristram-Nagle, S.; Liu, Y.; Legleiter, J.; Nagle, J. F. Structure of Gel Phase DMPC Determined by X-Ray Diffraction. *Biophys. J.* **2002**, *83*, 3324–3335.
- (25) Hughes, A. V.; Roser, S. J.; Gerstenberg, M.; Goldar, A.; Stidder, B.; Feidenhans'l, R.; Bradshaw, J. Phase Behavior of DMPC Free Supported Bilayers Studied by Neutron Reflectivity. *Langmuir* **2002**, *18*, 8161–8171.
- (26) Kučerka, N.; Nieh, M.-P.; Katsaras, J. Fluid phase lipid areas and bilayer thicknesses of commonly used phosphatidylcholines as a function of temperature. *Biochim. Biophys. Acta, Biomembr.* **2011**, *1808* (11), 2761–2771.